COO-3065-107

UR-517

MASTER

NEUTRAL BEAM STUDIES OF COHERENT PRODUCTION ON NUCLEI FROM GeV/c

BY

WILLIAM C. CARITHERS, JR.

THE UNIVERSITY OF ROCHESTER

DEPARTMENT OF PHYSICS AND ASTRONOMY

ROCHESTER, NEW YORK

DISCLAIMER

UR-517 COO-3065-107
Conf-740984--2

NEUTRAL BEAM STUDIES OF COHERENT PRODUCTION ON NUCLEI FROM 6-16 GeV/c*

William C. Carithers, Jr.
Department of Physcis and Astronomy
University of Rochester
Rochester, New York
Contract Number AT(11-1)-3065
January 20, 1975

*To appear in Proc. Topical Meeting on High Energy Collisions Involving Nuclei, ICTP, 9-13 September 1974.

NEUTRAL BEAM STUDIES OF COHERENT PRODUCTION ON NUCLEI FROM 6-16 GeV/c

William C. Carithers, Jr.
University of Rochester, Rochester, New York 14627

Introduction

Coherent production has always been interesting as a filter for certain exchange mechanisms. Particular amplitudes - such as Pomeron exchange - can be enormously enhanced in coherent production from nuclei and even electromagnetic amplitudes can compete in certain reactions. We have been studying reactions of the sort

$$n + A \to (p\pi^-) + A$$

$$K_L^o + A \to (K^-\pi^+) + A.$$

We have analyzed a small fraction of the data; and even though the results are very preliminary, many trends are clear. This report will consist of four parts: (1) a brief description of the experimental technique, (2) measurement of total cross-section for unstable $(p\pi^-)$ states in nuclear matter, (3) Coulomb production of $\Delta^o(1236)$ and $K^{*o}(890)$, (4) resonance prodution.

1. Experimental Details

The apparatus and target system are shown in Fig. 1. The neutral beam is taken at an 83mr production angle from the Brookhaven AGS internal target. It consists of approximately 95% neutrons and 5% K_L^o with a broad momentum spectrum ranging from 4-16 GeV/c. Data were taken with targets of C, Al, Cu, Cd, Pb, and U, each approximately 0.2 radiation lengths thick. The target was enclosed in an evacuated volume and surrounded by a veto system of scintillator-lead sandwiches to suppress incoherent interactions.

The spectrometer consists of 3 planes of proportional wire chambers, (PWC), a wide aperture magnet, and a threshold Cerenkov counter for identifying pions. Each PWC plane contains both X, Y readouts and each of these is divided into logically independent left and right halves in order to interpret the 2-prong topology without ambiguity.

The resolution of the apperatus was calibrated using $K_L^o \to \pi^+\pi^-$ decays. The mass and t' distributions are shown in Fig. 2. The mass resolution is 4 MeV/c^2 and the t' resolution is better than .00004 (GeV/c)^2. Multiple scattering in the target increases this somewhat, but the t' resolution is still capable of resolving Coulomb production. The beam flux was monitored using K decays so that all intensity-dependent corrections are automatically included.

The acceptance of the apparatus is smooth in both mass and t' with the exception of a sharp drop in acceptance for masses very close to threshold. This inefficiency arises from a requirement that both tracks have momenta above the Cerenkov counter pion threshold.

2. $(p\pi^-)$ Cross Section in $n + A \rightarrow (p\pi^-) + A$ [1]

We have interpreted our data within the framework of an optical model using essentially the same analysis techniques developed for multipion production in nuclei[2]. The differential cross section for production of $p\pi^-$ is written as the sum of a coherent part and an incoherent part:

$$\frac{d\sigma}{dt'dm} = C_o(m,p)\{A^2|\tilde{F}(t',m,p)|^2 + I_o(m,p,A)e^{-B(m,p)t'}\}$$

where $C_o(m,p) = \frac{d\sigma}{dt'dm}$ at $t' = 0$ for free nucleons

$I_o(m,p,A) =$ incoherent proportionality factor

$B(m,p) =$ slope parameter for free nucleons

The details of the optical model are contained in the form factor, $\tilde{F}(t',m,p)$. For completeness, we give the exact expressions:

$$\tilde{F}(t',m,p) = 2\pi\int_{-\infty}^{\infty}dz \int_{0}^{+\infty}db\ b\ \exp[i\ \frac{m^2 - m_n^2}{2p}\ z]J_o(\sqrt{t'}\ b)\rho(b,z)$$

$$\times \exp[-(1-i\alpha_1)\tfrac{1}{2}\sigma_1 T_1(b,z)]\ \exp[-(1-i\alpha_2)\tfrac{1}{2}\sigma_2 T_2(b,z)]$$

where

$$T_1(b,z) = \int_{-\infty}^{z} A\,\rho(b,z')dz',\quad T_2(b,z) = \int_{z}^{\infty} A\,\rho(b,z')dz'$$

$$\rho(r) = \rho_o[1 + \exp\frac{r-c}{a}]^{-1}\quad \text{(Fermi distribution)}$$

$\sigma_1(\sigma_2) =$ total cross section for incoming (outgoing) system

$\alpha_1(\alpha_2) =$ ratio of real to imaginary part of scattering amplitude for incoming (outgoing) system

Although the formulas are long, their interpretation is straightforward. The first exponential in $\tilde{F}$ is just the longitudinal coherence phase. The second and third exponents describe the complex (including absorption) indices of refraction for the incoming and outgoing systems. $T_1(T_2)$ are just the thickness functions for the incoming (outgoing) systems for a point interaction at impact parameter b and beam coordinate z. For this section we have not included Coulomb production terms so we restrict the mass of the $p\pi^-$ to be outside the region of the $\Delta^o(1236)$ where Coulomb effects are noticable.

The optical model parameters for the incoming system (neutron) and the nuclear density function have been very well measured. These are then fixed to be:

$\sigma_1 = 39$ mb [3]

$\alpha_1 = -0.3$ [4]

$c = 1.18$ fm $A^{1/3}$ [5]

$a = 0.545$ fm [6]

The slope parameter, $B = 11\ (\text{GeV/c})^{-2}$, is found by a fit to the data in the incoherent region $0.1 < t' < 0.3\ (\mathrm{GeV}/c)^2$, in reasonable agreement with hydrogen data.

First we show in Fig. 3 that the t' distributions for all the elements studied are well represented by the optical model where we have arbitrarily set $\sigma_2 = 39$ mb, $\alpha_2 = 0$. For Pb we observe the expected diffraction pattern out to the fourth maximum. No attempt was made to correct the model for experimental resolution.

Having shown that the model is applicable, we proceed to fit for σ_2 making use of the strong dependence of the coherent cross section of atomic numbers, A. One standard technique for extracting the coherent cross section uses the extrapolation of $d\sigma/dt'$ to $t' = 0$. This requires a detailed knowledge of the experimental resolution. We have chosen instead to integrate the coherent part in the interval $0 < t' < t'^*$, where t'^* is the second diffraction maximum for each target.

The results of the fit are shown in Fig. 4. We find $\sigma_2 = (36 \pm 7)$mb for the mass interval $1.35\ \mathrm{GeV} < m_{p\pi^-} < 1.45\ \mathrm{GeV}$ with a χ^2 of 4.5 for 5 degrees of freedom. The error corresponds to a unit change in χ^2. Lacking any wisdon on a choice for α_2, we have constrained it to zero. Changing α_2 to -0.3 leads to a decrease in σ_2 of 6 mb.

The value of σ_2 thus obtained confirms the previous observations of coherent production of multiparticle final states in nuclei.[7] The outgoing state is absorbed with about the same cross section as the incoming state.

3. Coulomb Production

Following the original suggestion of Primakoff[8] for measurement of the π^0 lifetime, several examples of "photoproduction" reactions have been studied using the virtual photons in the Coulomb field of a heavy nucleus as a target. This technique is especially important in the case of Vector meson → Pseudoscalar meson + γ, since these radiative widths are often very difficult to obtain by other means. The radiative widths for such reactions are related in the limit of SU_3 symmetry as listed in Table I.

We have looked for examples of the reaction $n + \gamma_c \to \Delta^0(1236) \to p\pi^-$. The cross section for this process can be related to the measured photoproduction cross section, σ_γ, as a check on the Primakoff process:

$$\frac{d^2\sigma}{dt\,dm^*} = \frac{z^2\alpha}{\pi}\ \frac{\sigma_\gamma}{(m^{*2} - m^2)}\ \frac{t'}{t^2}\ |F(t)|^2$$

First we show the general features of the $p\pi^-$ mass distribution for a Pb target integrated over all t', in Fig. 5. The distribution is broad and featureless with the possible exceptions of enhancements in the regions of the $\Delta(1236)$ and $N^*(1690)$. If the $\Delta(1236)$ is due to Coulomb production, it should be seen only for very small t', ($t' < .002\ \mathrm{GeV}/c^2$) and only for large Z^2. In Fig. 6 we show mass distributions for a Pb target for various t' cuts. For $t' < .001\ \mathrm{GeV}/c^2$ the Δ is the most prominant feature. For the region $.001 < t' < .006\ \mathrm{GeV}/c^2$, some Δ remains but no evidence for Δ is seen for $t' > .006\ \mathrm{GeV}/c^2$. The corresponding distributions for a C target are shown in Fig. 7. No evidence for the Δ is seen, although otherwise the shape of the mass distribution is essentially the same as the Pb data. In fact, a careful Pb–C difference gives a clean Δ signal in reasonable agreement with expectations for Coulomb production.

Thus encouraged, we searched for examples of the reaction $K_L^0 + \gamma_c \rightarrow \bar{K}^{*0}(890) \rightarrow K^-\pi$. Unlike the Δ which requires isovector exchange, this reaction proceeds via isoscalar (presumably ω) exchange. The Coulomb process must be then extracted from a strong background of ω-exchange. The differential cross section for Coulomb production is expected to be of the form:

$$\frac{d\sigma}{dt} = 24\pi Z^2\alpha \quad \Gamma(\bar{K}^{*0} \rightarrow \bar{K}^0\gamma) \frac{m^{*3}}{(m^{*2} - m^2)^3} \frac{t'}{t^2} |F(t)|^2$$

This Coulomb contribution peaks at very small t' ($t' = .0005$ GeV/c^2) whereas the ω exchange is much broader and peaks at larger t' ($t' = .002$ GeV/c^2). Both contributions must go to zero as $t' \rightarrow \infty$ as a consequence of parity conservation (helicity-flip amplitudes).

The mass distribution for $K^-\pi^+$ events from a Pb target is shown in Fig. 8. A clear K*(890) signal is found both for all t' and for $t' < .006$ GeV/c^2 where the Coulomb signal is enhanced. The t' distribution for $.84 < m_{K\pi} < .94$ GeV is shown in Fig. 9. The excess of events near $t' = 0$ is evidence for Coulomb production. The statistics at this time are not sufficient to determine the radiative width without knowledge of the relative phase between the Coulomb and ω-exchange terms. However, it is already clear that the radiative width is substantially smaller than one would expect based on unitary symmetry predictions with the measured $\Gamma(\omega \rightarrow \pi^0\gamma)$ as input. Such a conclusion does not disagree with recent results on $\Gamma(\rho \rightarrow \pi\gamma)$.[9]

4. Resonance Production

As previously noted, the $p\pi^-$ mass distribution shows a noticable structure in the region of the N*(1690). This structure seems to be a very general feature in our data and we list some of the systematic trends:

1. The structure appears in data from all nuclei studied, although it is more prominant in light nuclei. (Compare Figures 6 and 7.)
2. The structure at 1690 is more prominent for large t'. This is especially clear in Fig. 7.
3. There is a suggestion that the t' distribution is broader in the region of the 1690 than that obtained from lower masses. These t' distributions are shown in Fig. 10. Notice that the first diffraction minimum is almost completely washed out for masses in the structure at 1690.

Taken together these trends indicate that the structure at 1690 has a much larger incoherent component.

The analysis on all phases of the work reported here is continuing and we expect to increase the statistics by as much as 20-fold in the near future. It is a pleasure to acknowledge the contributions of my colleagues Dave Ryan of McGill, Tom Ferbel and Dave Underwood at Rochester, and particularly Peter Mühlemann at Rochester who has carried out most of the analysis.

Footnotes

1. W. C. Carithers et al., Contribution No. 454, XVII International Conf. on High Energy Physics, London, 1974.
2. K. S. Kolbig and B. Margolis, Nuc. Phys. B6, 85 (1968); C.Bemporad, et al., Nuc. Phys. B33, 397 (1971); Nuc. Phys. B42, 627 (1972); Nuc. Phys. B59, 106 (1973).
3. K. J. Foley et al., Phys. Rev. Lett. 19, 857 (1967); J. Engler, et al., Phys. Letters 27B, 599 (1968).
4. G. G. Beznogikh, et al., submitted to Yadenaja Fysika.
5. G. Belletini, et al., Nuc. Phys. 79, 609 (1966).
6. B. Hahn et al., Phys. Rev. 101, 1131 (1956).
7. See for example, C. Bemporad et al., op. cit.
8. H. Primakoff, Phys. Rev. 81, 899 (1951).
9. Leo Strawczynski, Thesis, University of Rochester Report UR-475.

TABLE I

Exact SU(3) Predictions for Radiative Amplitudes

$$- \langle K^{*0} | K^0 \gamma \rangle = \frac{2}{\sqrt{3}} \langle \omega_8 | \pi\gamma \rangle$$

$$= 2 \langle \rho | \pi\gamma \rangle$$

$$= 2 \langle K^{*+} | K^+ \gamma \rangle$$

$$= \frac{2}{\sqrt{3}} \langle \rho^0 | \eta\gamma \rangle$$

Ref: Becchi and Morpugo, Phys. Rev. 140B, 687

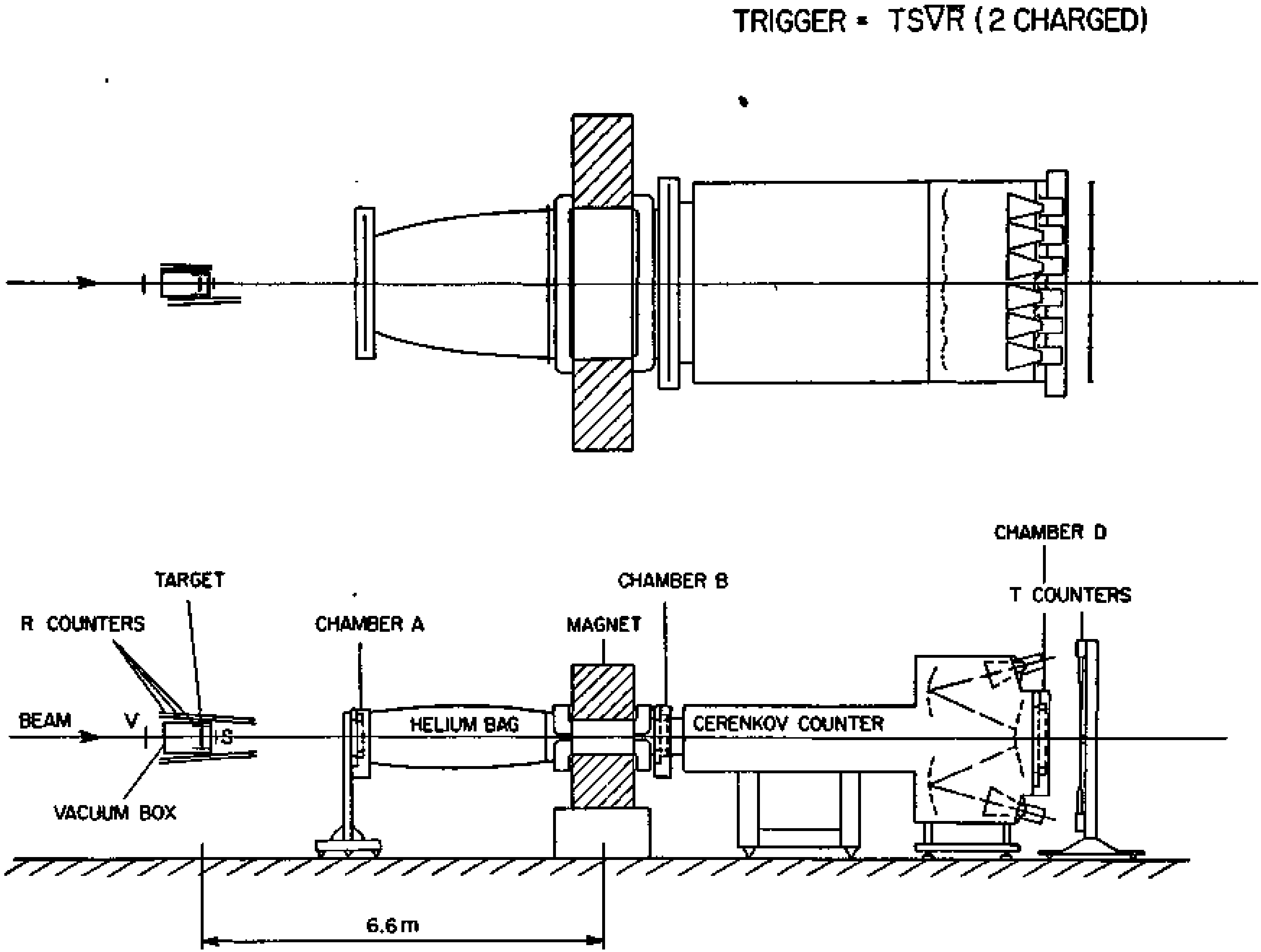
TRIGGER = TS$\bar{V}\bar{R}$ (2 CHARGED)
CHAMBER D
TARGET
CHAMBER B
T COUNTERS
R COUNTERS
CHAMBER A
MAGNET
BEAM
V
S
HELIUM BAG
CERENKOV COUNTER
VACUUM BOX
6.6 m

Figure 1

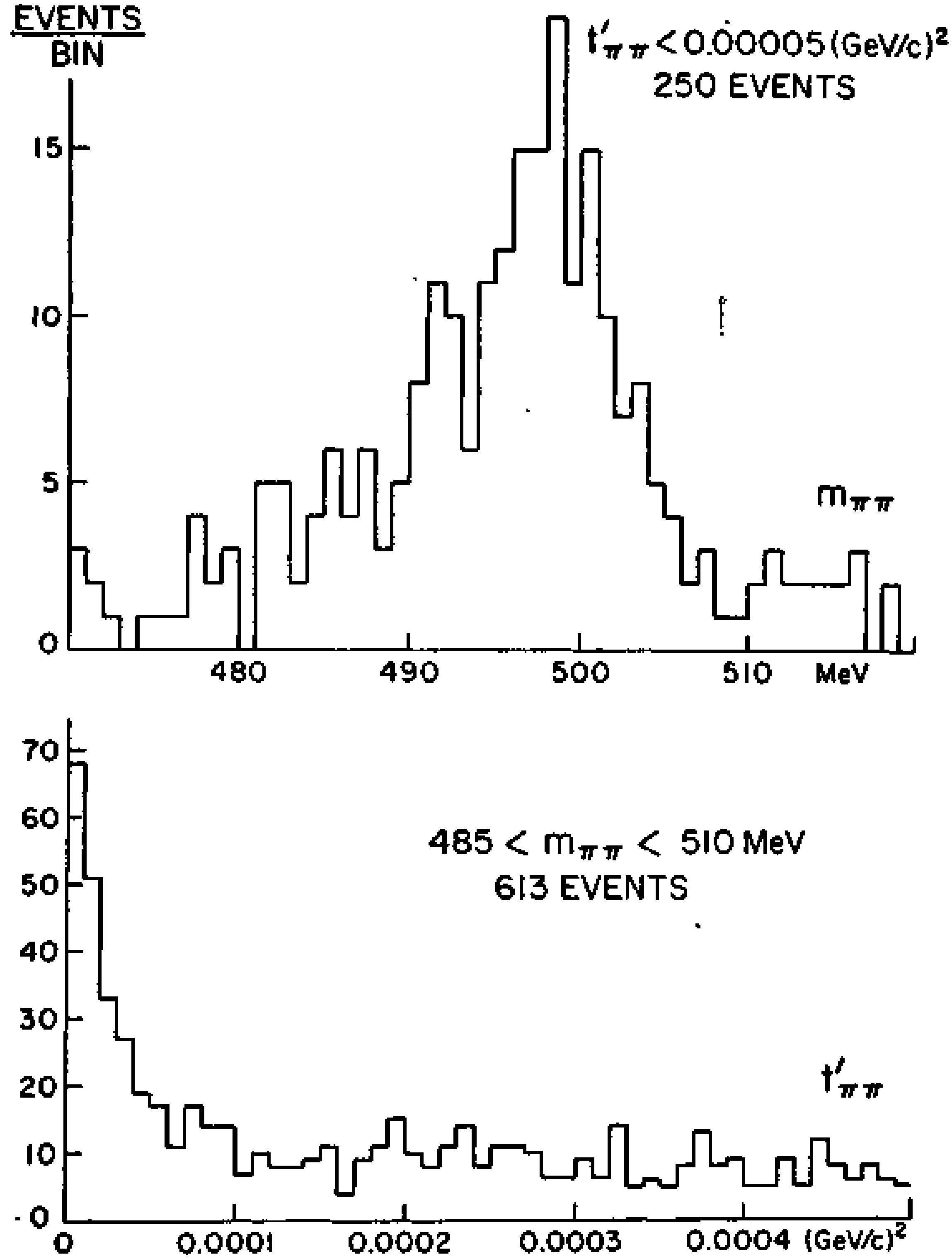
EVENTS
BIN
$t'_{\pi\pi} < 0.00005 (GeV/c)^2$
250 EVENTS
15
10
5
0
480
490
500
510
MeV
$m_{\pi\pi}$
70
60
50
40
30
20
10
0
$485 < m_{\pi\pi} < 510$ MeV
613 EVENTS
$t'_{\pi\pi}$
0
0.0001
0.0002
0.0003
0.0004 $(GeV/c)^2$

Figure 2

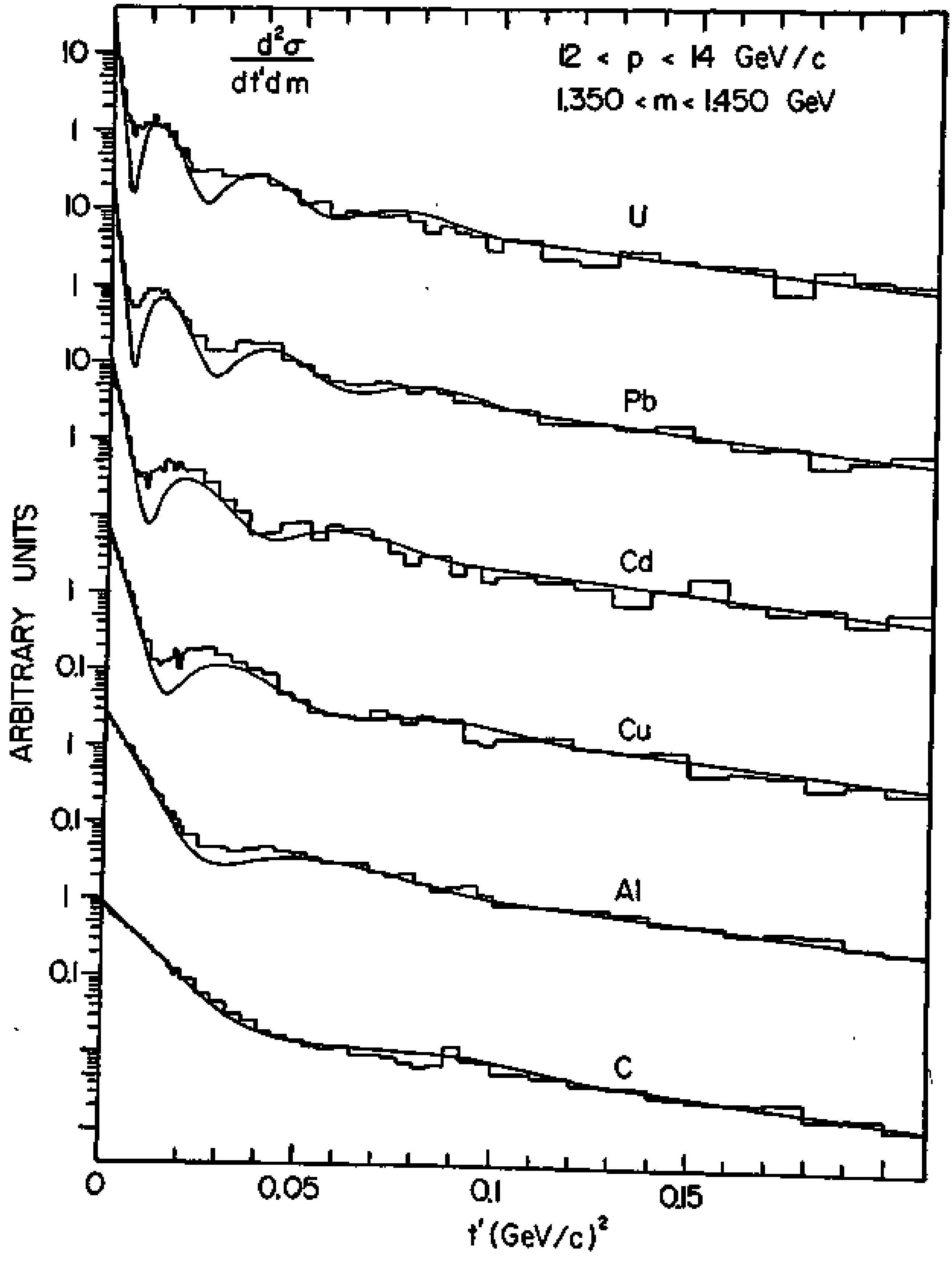

$\frac{d^2\sigma}{dt'dm}$
12 < p < 14 GeV/c
1.350 < m < 1.450 GeV
U
Pb
Cd
Cu
Al
C
ARBITRARY UNITS
10
1
0.1
0
0.05
0.1
0.15
t' (GeV/c)²

Figure 3

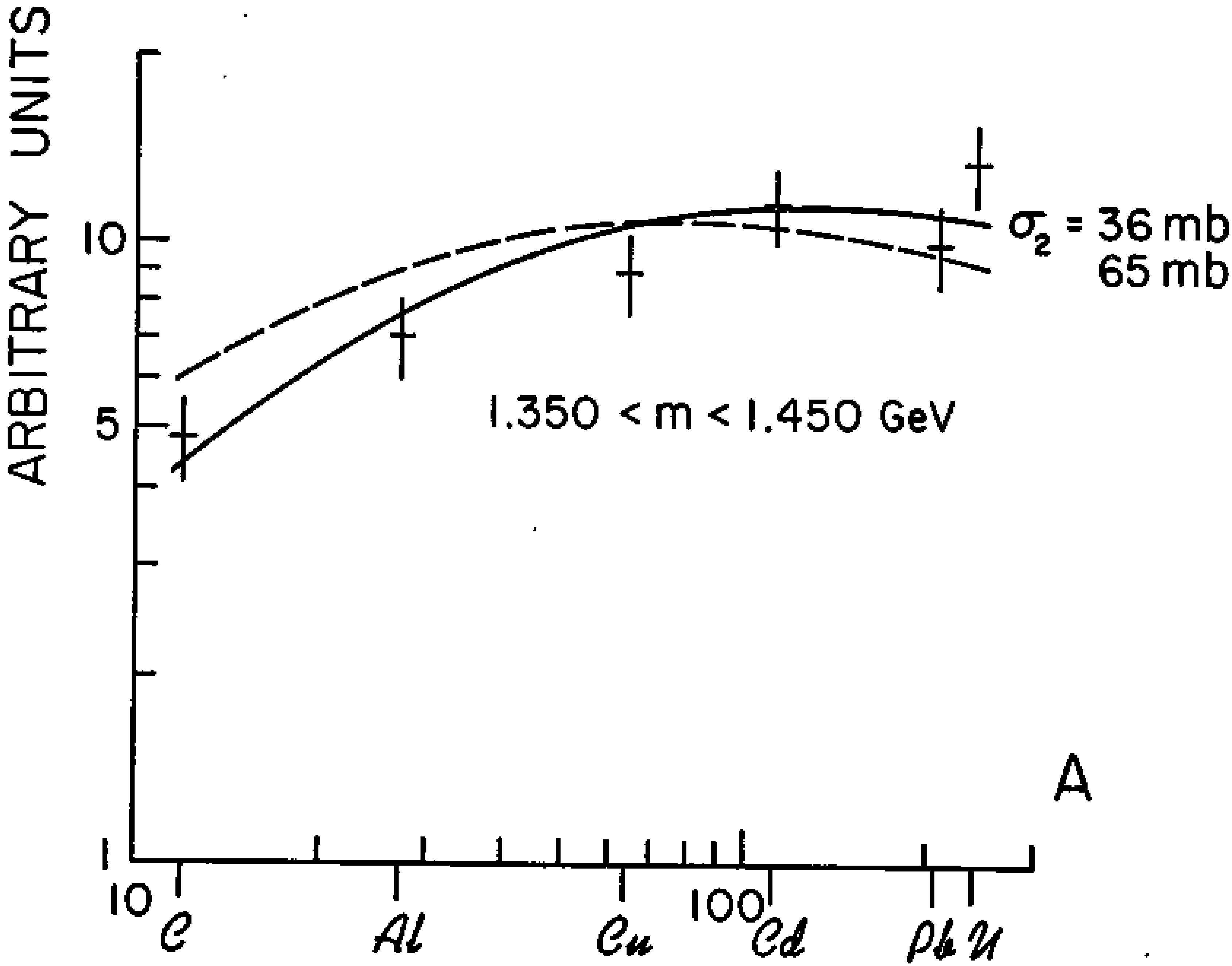
ARBITRARY UNITS
10
5
1
σ_2 = 36 mb
65 mb
1.350 < m < 1.450 GeV
A
10
100
C
Al
Cu
Cd
Pb
U

Figure 4

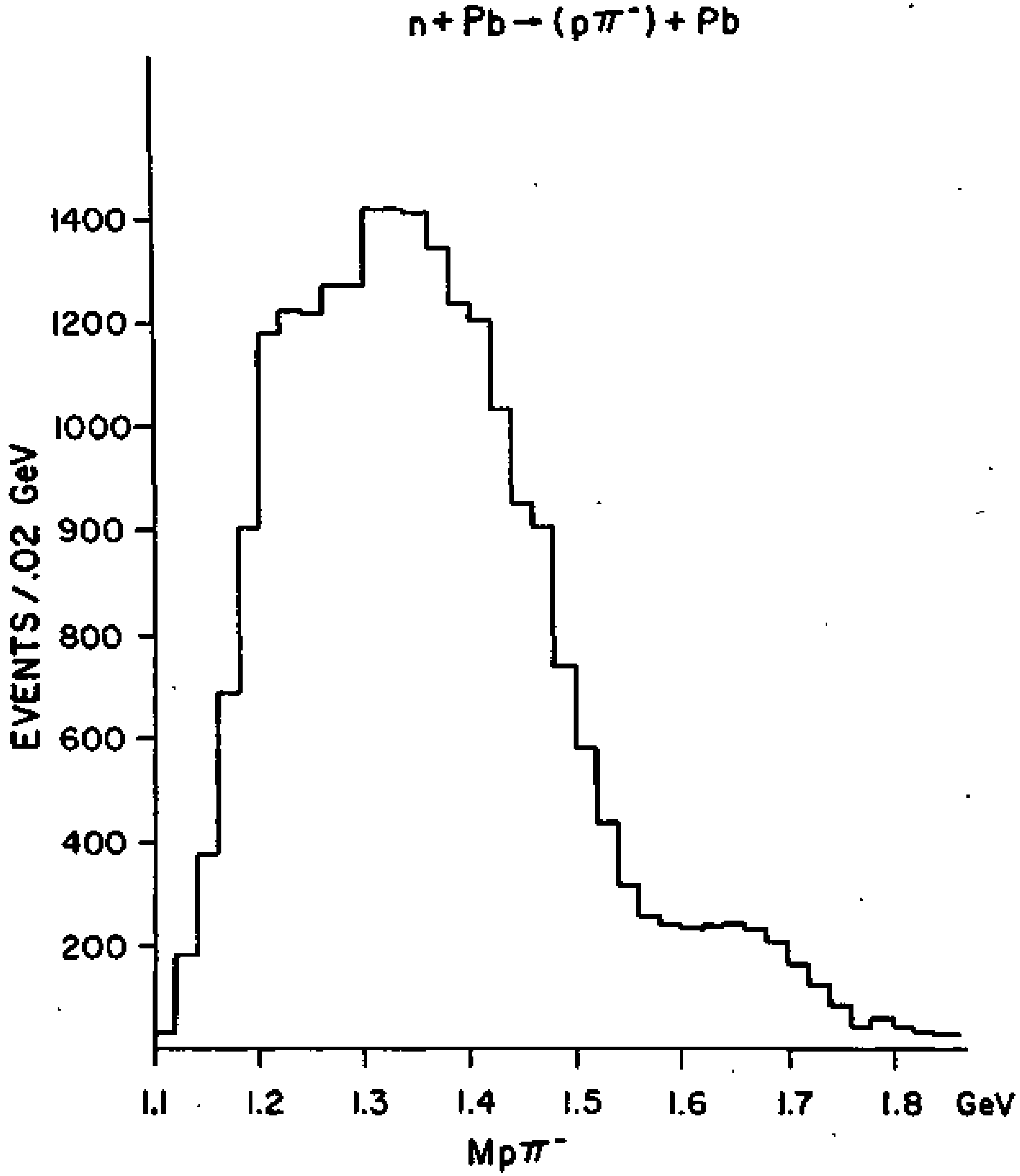
n + Pb → (pπ⁻) + Pb
1400
1200
1000
900
800
600
400
200
EVENTS / .02 GeV
1.1
1.2
1.3
1.4
1.5
1.6
1.7
1.8
GeV
Mpπ⁻

Figure 5

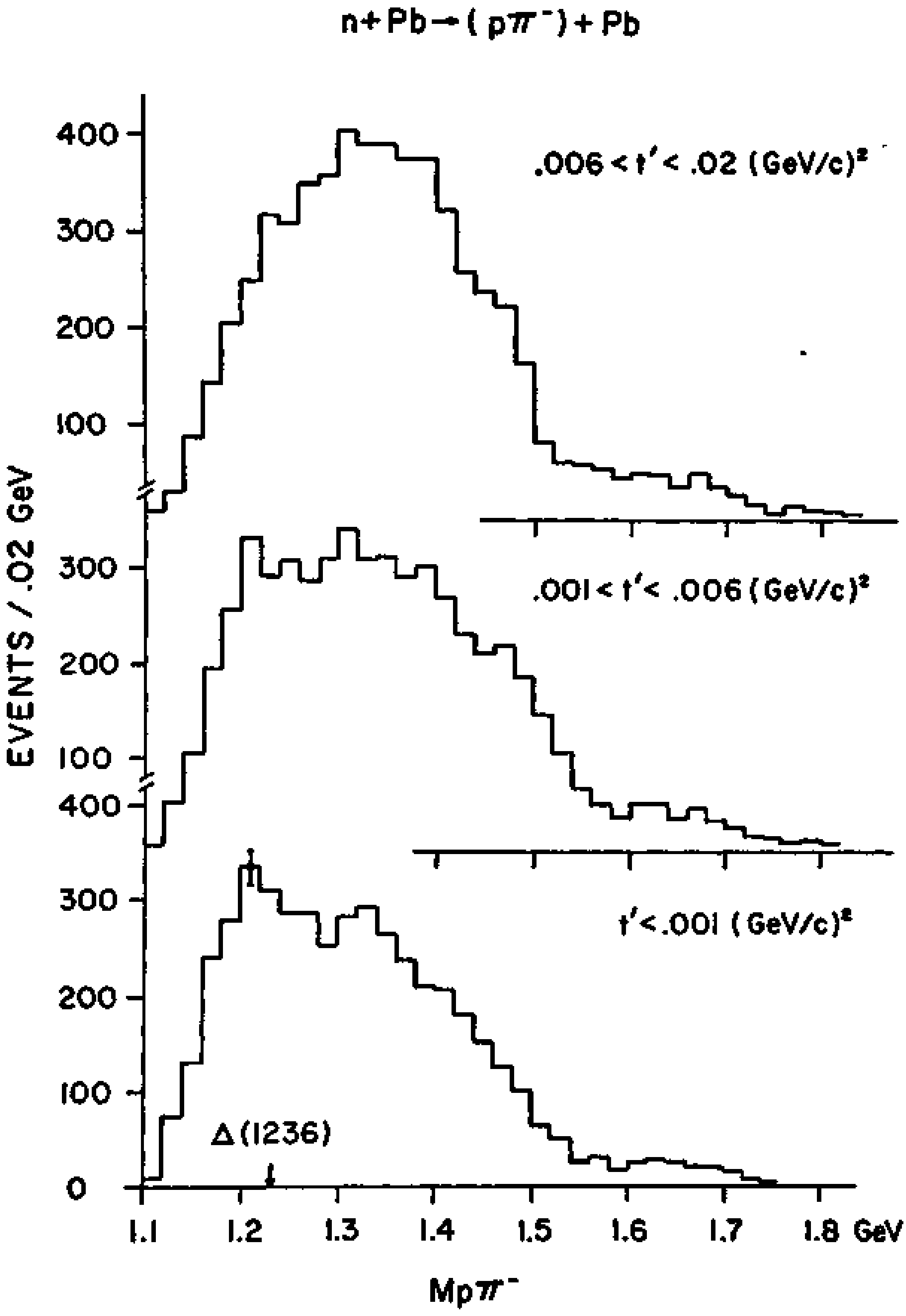
n+Pb→(pπ⁻)+Pb
.006 < t′ < .02 (GeV/c)²
.001 < t′ < .006 (GeV/c)²
t′ < .001 (GeV/c)²
EVENTS / .02 GeV
400
300
200
100
0
Δ(1236)
1.1
1.2
1.3
1.4
1.5
1.6
1.7
1.8 GeV
Mpπ⁻

Figure 6

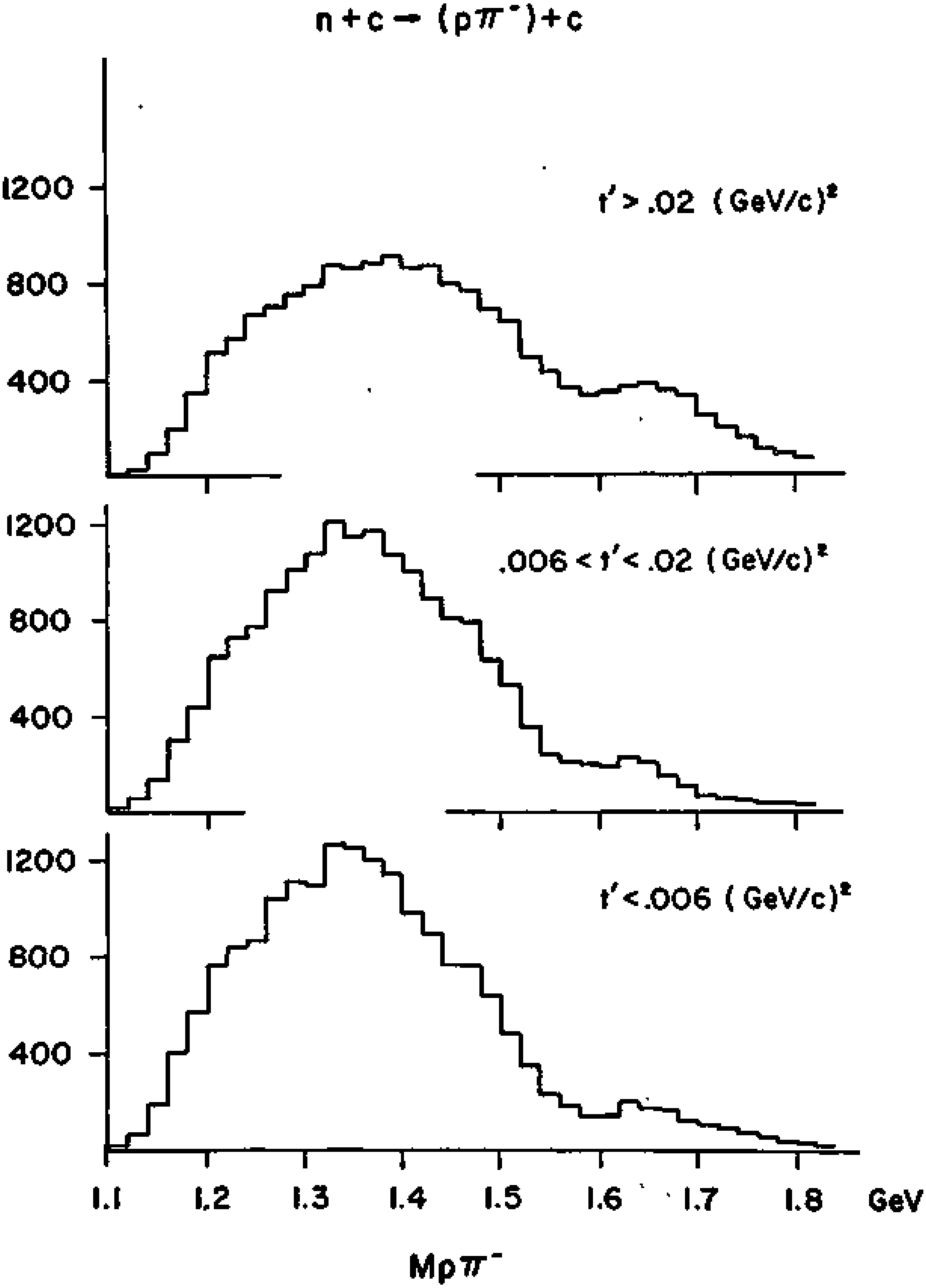
n + c → (pπ⁻) + c
1200
800
400
t' > .02 (GeV/c)²
.006 < t' < .02 (GeV/c)²
t' < .006 (GeV/c)²
1.1
1.2
1.3
1.4
1.5
1.6
1.7
1.8
GeV
Mpπ⁻

Figure 7

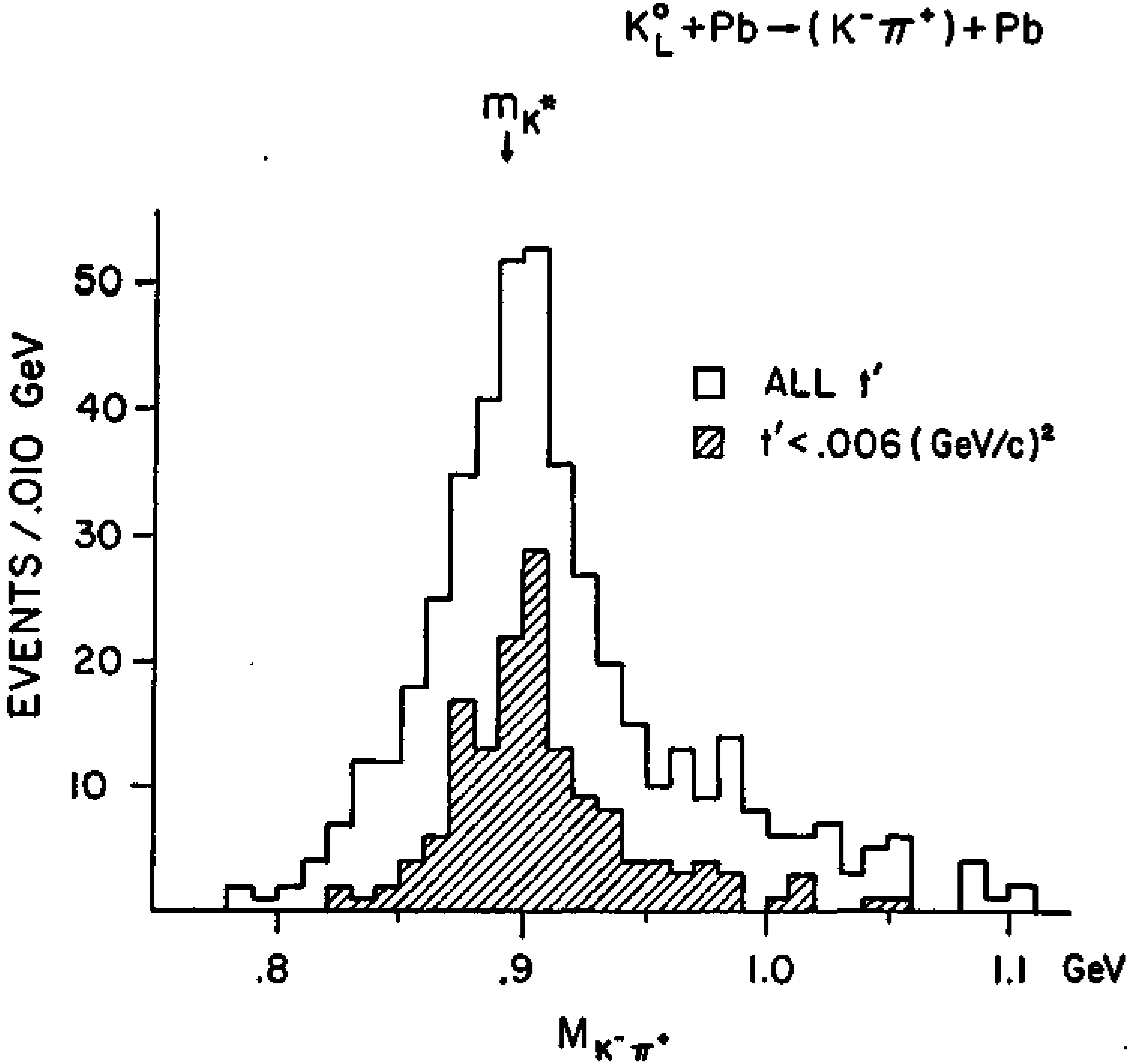
$K_L^o + Pb \rightarrow (K^- \pi^+) + Pb$
m_{K^*}
EVENTS / .010 GeV
50
40
30
20
10
ALL t'
t' < .006 (GeV/c)²
.8
.9
1.0
1.1 GeV
$M_{K^- \pi^+}$

Figure 8

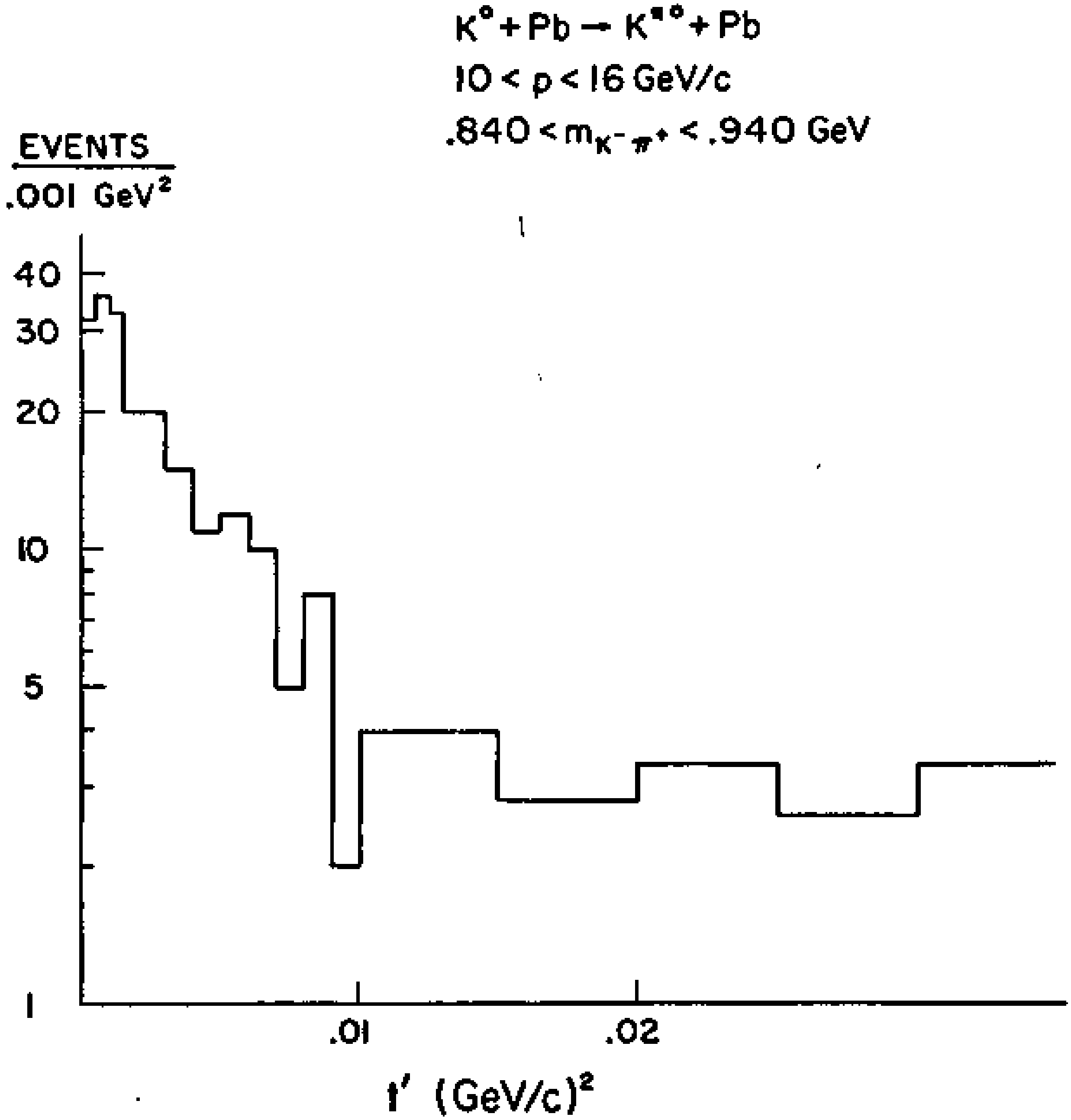
K° + Pb → K*° + Pb
10 < p < 16 GeV/c
.840 < m K⁻π⁺ < .940 GeV
EVENTS / .001 GeV²
40
30
20
10
5
1
.01
.02
t′ (GeV/c)²

Figure 9

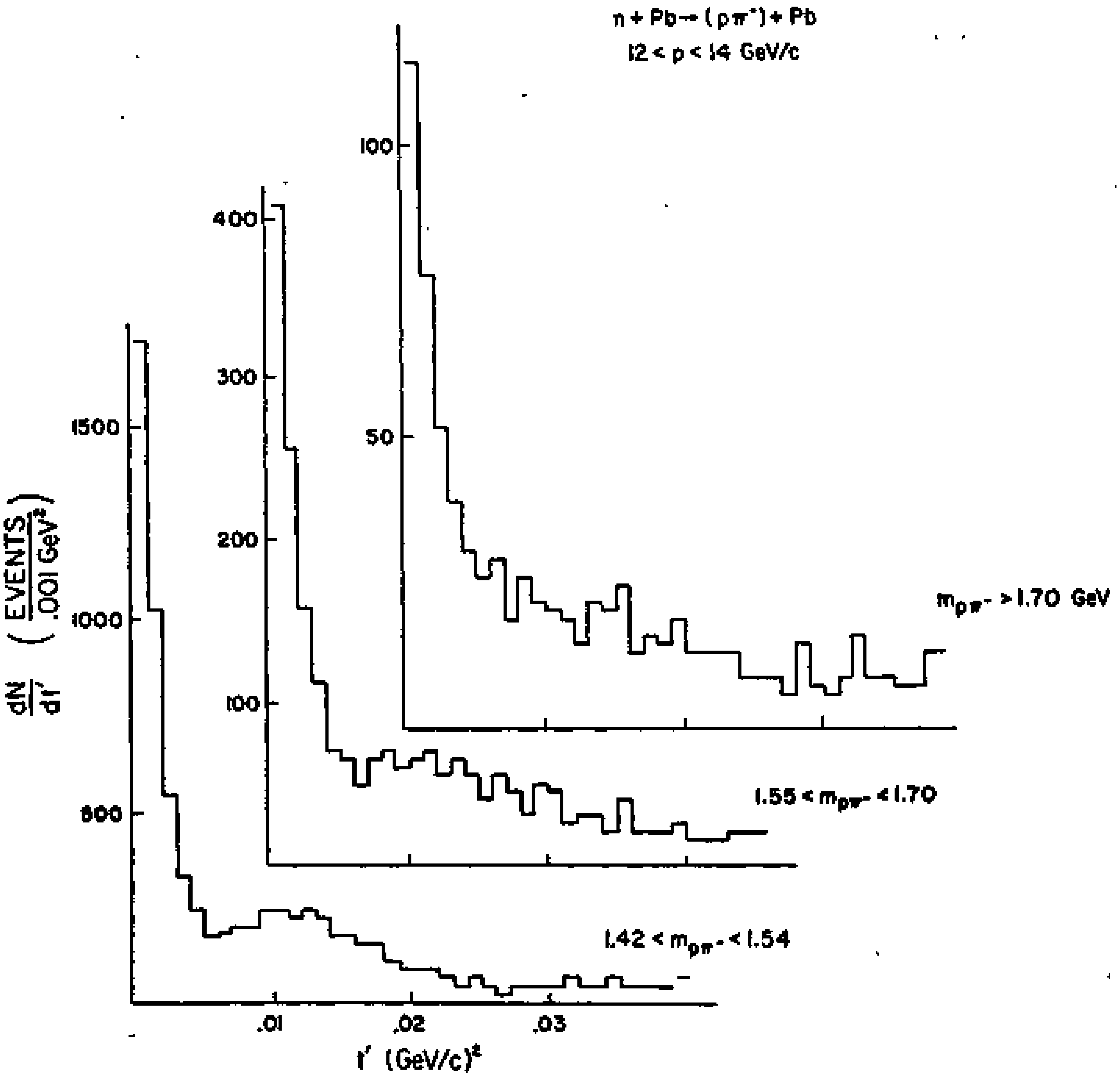
n + Pb → (pπ⁻) + Pb
12 < p < 14 GeV/c
100
50
400
300
200
100
1500
1000
500
dN/dt′ (EVENTS/.001 GeV²)
m_pπ⁻ > 1.70 GeV
1.55 < m_pπ⁻ < 1.70
1.42 < m_pπ⁻ < 1.54
.01
.02
.03
t′ (GeV/c)²

Figure 10